4 Chemical Properties of Poly(lactic Acid)

Chapter Outline

4.1 Introduction

Poly(lactic acid) (PLA) is known to be biocompatible and biodegradable, and it can be readily broken down by a hydrolysis reaction. PLA is derived from renewable agricultural resources, such as corn and cassava. Mass production of PLA can lead to high consumption of agricultural yields, which increases the farm economy. Moreover, the production of PLA helps to reduce CO_2 emissions when used in place of conventional petroleum-based commodity plastics, as the agricultural activities involve significant carbon fixation.

PLA is a biodegradable polymer that has been widely studied and is used for domestic packaging, and biomedical applications, such as resorbable sutures, surgical implants, scaffolds for tissue engineering and controlled drug-delivery devices. PLA can exist as two stereoisomers, designated as D and L, or as a racemic mixture, designated as DL. The D and L forms are optically active while the DL form is optically inactive. Poly(L-lactic acid) (PLLA) and poly(D-lactic acid) (PDLA) are semicrystalline,

Polylactic Acid. DOI: http://dx.doi.org/10.1016/B978-1-4377-4459-0.00004-4

while poly(DL-lactic acid) (PDLLA) is amorphous (Jain, 2000; Urayama et al., 2003).

PLA belongs to the family of aliphatic polyesters commonly made from α−hydroxyl acids, which also includes polyglycolic acid (PGA), polycaprolactone and polydioxanone. It is one of the few polymers that has a stereochemical structure that can be easily modified by polymerizing a controlled mixture of L and D isomers to yield a high-molecular-weight and amorphous or semicrystalline polymer. The properties of PLA can be modified both through the variation of isomers (L/D ratio) as well as copolymerization with other monomers, such as glycolide and caprolactone. PLA can also be tailored by formulation involving the addition of plasticizers, other biopolymers and fillers. The biodegradability of PLA blends means that they are well suited for short-term packaging materials, and they also further expand PLA's applications in the biomedical field, where biocompatible characteristics are essential, such as implants, sutures and drug encapsulations.

In the early days of PLA development, PLA was produced using the polycondensation method (see Figure 4.1). This was the most direct method of synthesizing PLA but the drawback was

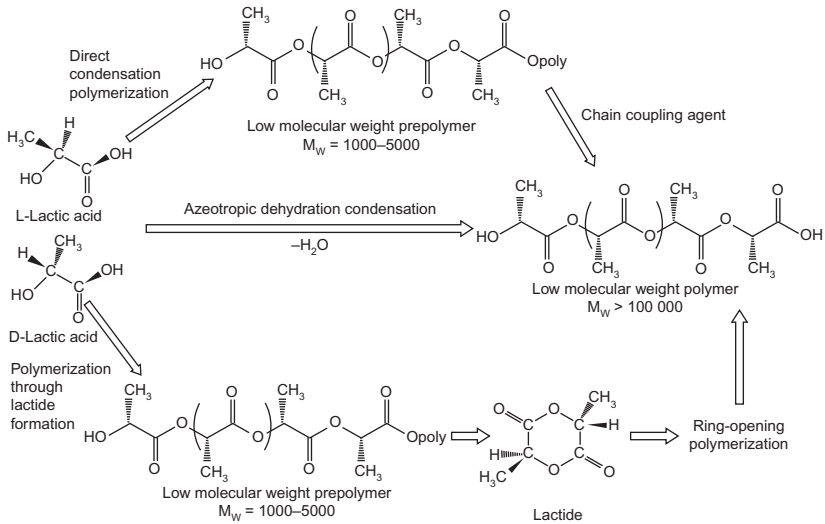

Figure 4.1 Routes for synthesis of poly(lactic acid) (adapted from Hartmann et al., 1998).

the generation of excessive water and a low-molecular-weight ($M_n < 1000-5000$ Da) product. Sometimes, a chain extender may be needed to increase the molecular weight, but this results in a higher cost of production. PLA also can be produced using the azeotropic dehydrative condensation approach. This polymerization technique yields high-molecular-weight polymers, but requires various diacids, diols, or hydroxyl acids as well as high-level catalysts (Garlotta, 2002). All these ingredients remain as impurities in the PLA and may initiate unwanted degradation during subsequent processing work at elevated temperatures.

The most important method for mass production of high-molecular-weight PLA is through the ring-opening polymerization approach. High-molecular-weight PLA is produced from the cyclic dilactate ester (commonly known as lactide), which commonly involves the action of stannous octoate as a catalyst. This mechanism does not generate additional water, hence, a higher molecular weight can be achieved. Polymerization of a racemic mixture of L- and D-lactides usually leads to the synthesis of PDLLA, which is amorphous. The utilization of stereospecific catalysts tends to produce stereochemically pure PLA with good crystallinity. The degree of crystallinity and the physicomechanical properties are greatly determined by the ratio of D to L enantiomers, which is also partially related to the types of catalyst used. It has been reported that high-quality production of PLA yields a minimum amount of unreacted lactic acid monomer, which limits the tendency of lactic acid to leach out from the PLA when using as packaging. Furthermore, the amount of leached lactic acid is very much lower compared to the amount of lactic acid in common food ingredients (Mutsuga et al., 2008). Therefore, polymers derived from lactic acid can be good candidates for packaging applications (Iwata and Doi, 1998). PLA has been growing as an alternative packaging material for niche markets. Currently, PLA is used as a food packaging polymer for short-shelf-life consumer products, including containers, drinking cups, razors and stationery. PLA fibers are also used in carpet, sportswear and diapers. A number of new applications have been developed in recent years, such as casing for electronic devices, flooring materials, etc. The ‘green’ credentials of

PLA means there is a sustainable future for plastic materials globally.

4.2 Stereochemistry of Poly(lactic Acid)

The basic ingredient of PLA is lactic acid, which is yielded from bacterial fermentation or from a petrochemical source. Lactic acid is a naturally occurring substance with the standard chemical name 2-hydroxy propionic acid. It is the simplest hydroxyl acid with an asymmetric carbon atom, and has optically active L(+) and D(−) isomers. Both L and D isomers are produced in bacterial systems, with the L isomer more commonly found. Meanwhile, mammalian systems produce only the L isomer, which is easily assimilated by enzyme protease K. Figure 4.2 shows the chemical structure of the L- and D-lactic acids.

Nowadays, lactic acid is mass produced through the bacterial fermentation of carbohydrates, where corn and cassava are the main agricultural sources. There are about 20 genera in the phylum Firmicutes that generate lactic acid; these include *Lactococcus*, *Lactobacillus*, *Streptococcus*, *Leuconostoc*, *Pediococcus*, *Aerococcus*, *Carnobacterium*, *Enterococcus*, *Oenococcus*, *Tetragenococcus*, *Vagococcus* and *Weisella* (Reddy et al., 2008). Strains of *Lactobacillus delbrueckii*, *Lactobacillus jensenii*, and *Lactobacillus acidophilus* produce D-lactic acid and some also produce mixtures concurrently (Nampoothiri et al., 2010). Many fermentation processes nowadays use a species of *Lactobacillus* that has a higher yield of lactic acid. These bacteria can actively produce lactic acid under broad processing conditions, including a pH of 5.4−6.4, temperatures of 38−42°C, and they survive in a low oxygen concentration. Often agricultural sources of simple sugars, such as glucose and

Figure 4.2 Chemical structures of L- and D-lactic acid with a melting point of 16.8°C.

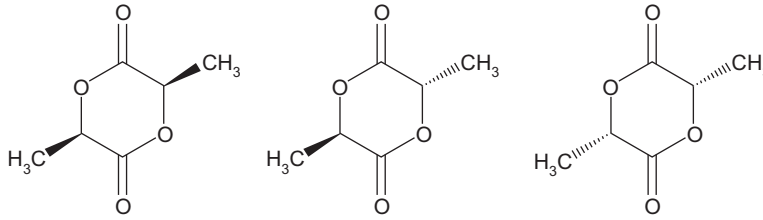

Figure 4.3 Chemical structures of L,L-, meso- and D,D-lactides (m.p. is melting point).

maltose from corn or potato, sucrose from cane or beet sugar, and lactose from cheese whey are widely used for lactic acid fermentation. Other nutrients, such as vitamin B complex, amino acids and nucleotides are needed to ensure functionality of the bacteria throughout the process; such a nutrient package can be provided by a rich corn-steep liquor.

Polymerization through lactide formation is the current method employed by NatureWorks® to produce high-molecular-weight PLA polymers for commercial applications. The lactide is the cyclic dimer of lactic acid, and is the intermediate product for ring-opening polymerization of PLA. A step is taken to prepolymerize either D-lactic acid, L-lactic acid or a mixture of the two, to obtain intermediate lactic acid oligomers (chains of $<$1000 lactic acid repeating units) and this is followed by a catalytic reaction under lower pressure to depolymerize and obtain a mixture of lactide stereoisomers. There are three stereoforms of lactide, the cyclic dimer of lactic acid, which is built up from a condensation reaction of two lactic acid molecules as follows: L-lactide (two L-lactic acid molecules), D-lactide (two D-lactic acid molecules) and meso-lactide (an L-lactic acid and a D-lactic acid molecule) as shown in Figure 4.3. According to Hartmann (1998), the formation of different percentages of the lactide isomers can be affected by the lactic acid isomer feedstock, the temperature and the catalyst. The lactide undergoes vacuum distillation for optical purification and this is followed by bulk melt polymerization to produce high optically pure PLA. Commercial manufacturers prefer bulk melt polymerization because it involves lower levels of nontoxic catalysts, such

as less-reactive metal carboxylates, oxides, and alkoxides. These work to assist in synthesizing a high-molecular-weight PLA. It has been observed that lactides easily undergo polymerization in the presence of transition metals (tin, zinc, aluminum, etc.) with tin (II) and zinc having the ability to yield the purest polymers. Some studies have reported that these catalysts are more effective in lactide polymerization because of the covalent metal−oxygen bonds and free *p* or *d* orbitals (Kricheldorf and Boettcher, 1993; Dahlman et al., 1990).

As mentioned, lactic acid is a chiral molecule possessing L and D isomers, and the composition of the lactic acid in terms of these two isomers significantly affects the characteristics of the PLA. This means that the stereochemistry of PLA may be tailored to fit its applications. It is the stereoregularity of the built-up monomers that determines PLA as a highly crystalline polymer (Huang et al, 1998). Stereochemically pure PLA of either D-lactic acid or L-lactic acid can be a crystalline polymer. Amorphous materials can be made by the inclusion of relatively high D or L content (>20%), whereas highly crystalline materials can be obtained when the D or L content is low (<2%) (Lunt and Shafer, 2000). Hence, PLA can be made up of the three stereoisomers of lactide: L-lactide, D-lactide, and meso-lactide; depending on the constituents, the resulting polymer can have varying characteristics. The stereochemical composition of the polymer has a dramatic effect upon the melting point of the polymer, the rate of crystallization and the ultimate extent of crystallization. According to Drumlight et al. (2000), PLA made from pure L-lactide, also called poly(L-lactide), has an equilibrium melting point of 207°C and a glass transition temperature of about 60°C. Commonly, high stereochemically pure PLA, either in L or D, possesses a melting point of around 180°C with an enthalpy of melting of 40−50 J/g. Subsequent introduction of irregularity of stereochemistry in the polymer, such as by copolymerization of poly(L-lactide) with meso-lactide or D-lactide, can cause a significant reduction in melting point (see Figure 4.4), rate of crystallization and extent of crystallization, but it has no effect on the glass transition temperature (Lunt, 1998). From a study conducted by Kolstad (1996), it was

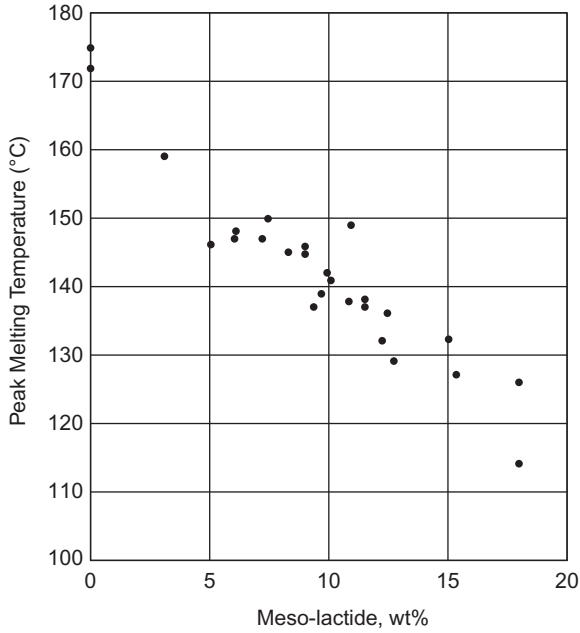

Figure 4.4 Peak melting temperature of poly(L-lactide-co-meso-lactide) (adapted from Kolstad, 1996).

recognized that the peak melting temperature reduced in a roughly proportional manner. The crystallization half-time of the copolymer increased significantly for a high-meso-lactide content version (see Table 4.1). Higher average molecular weight causes the recrystallization time to increase several-fold. These findings were further strengthened by Huang et al. (1998), who found that spherulitic growth rates were strongly dependent on meso- content as well. The degree of crystallinity of the poly(L-lactide-co-meso-lactide) copolymer exhibits a dramatic drop with increasing D isomer content (D-isomer contributed by meso-lactide), ranging from 40−60% for poly(L-lactide) to values <20% for copolymer with 12% meso- content (or containing 6.6% D isomer), as shown in Figure 4.5. The melting point and glass transition data for selected PLA structures and blends are summarized in Table 4.2 (Henton et al., 2005).

Pure crystal of PLA, i.e. 100% crystallinity, has the theoretically enthalpy of melting (ΔH_m) of 93.7 J/g as compared to the experimental values 40−50 J/g for a polymer with 37−47%

Table 4.1 Crystallization Half-Time (Min) for Poly(L-lactide-co-meso-lactide) (Kolstad, 1996)

Temperature (°C)	0% Meso-		3% Meso-		6% Meso-	
	M_n = 101,000	M_n = 157,000	M_n = 88,000	M_n = 1 14,000	M_n = 58,000	M_n = 114,000
85	14.8	–	23.9	–	–	–
90	7.0	11.4	11.0	–	–	–
95	4.5	–	8.1	–	–	–
100	3.8	4.8	9.4	11.4	27.8	–
105	2.9	–	8.6	–	19.6	–
110	1.9	4.0	6.0	10.8	19.7	44
115	3.5	–	6.9	–	22.2	–
120	4.0	5.7	8.2	11.6	–	–
125	5.1	–	11.5	–	–	–
130	8.7	13.4	–	–	–	–
135	22.9	–	–	–	–	–

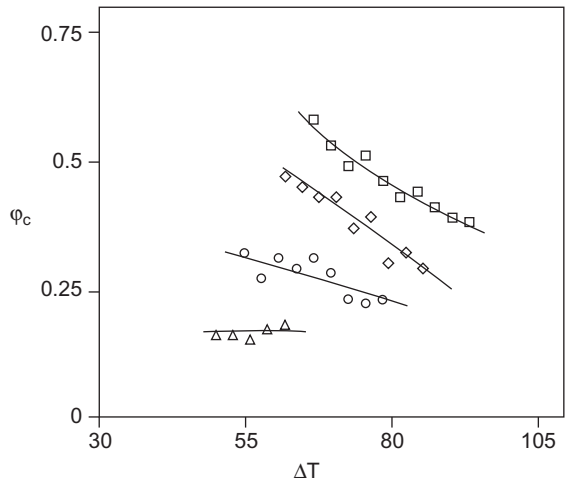

Figure 4.5 Bulk degrees of crystallinity (φ_c) as a function of degree of supercooling ($\Delta T = T_m^{\circ} - T_x$, where T_m° is the equilibrium melting point and T_x is isothermal crystallization temperature) of poly(L-lactide-co-meso-lactide). □ = 0% meso-lactide with 0.4 D-isomer content; ◇ = 3% meso-lactide with 2.1% D-isomer content; ○ = 6% meso-lactide with 3.4 isomer content; △ = 12% meso-lactide with 6.6% D-isomer content (adapted from Huang et al., 1998).

Table 4.2 The Effects of Stereochemistry of PLA on Melting Point and Glass Transition

Structure	Description	T_m (°C)	T_g (°C)
Isotactic poly(L-lactide) or poly(D-lactide)	~LLLLLL~ or ~DDDDDD~	170–190	55–65
Random optical copolymers	Random level of meso- or D-lactide in L-lactide or D-lactic acid in L-lactic acid	130–170	45–65
PLLA/PDLA stereocomplex	~LLLLLL~ blended with ~DDDDDD~	220–230 (Ikada et al., 1987)	65–72 (Tsuji and Ikada, 1999)
PLLA/PDLA stereoblock complexes	~LLLLLL~DDDDDD~	205 (Yui et al., 1990)	40 (Ovitt and Coates, 1999)
Syndiotactic poly(meso-) PLA	~DLDLDLDLDL~ Al-centered R-chiral catalyst	179 (Ovitt and Coates, 2000) 152 (Ovitt and Coates, 1999)	
Heterotactic-(disyndiotactic) poly(meso-lactide)	~LLDDLLDDLLDDLLDD~ Al-centered *rac*-chiral catalyst		40 (Ovitt and Coates, 1999)

Adapted from Henton et al., 2005.

crystallinity (Tsuji and Ikada, 1995; Tsuji and Ikada 1996). It is important to note that the extent of crystallization can be varied according to the rate of cooling, polymerization conditions and the presence of impurities or enantiomers. Huang et al. (1998)

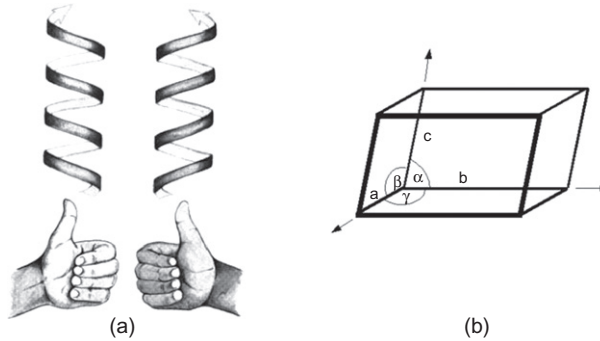

Figure 4.6 (a) Left-hand and right-hand helices (Morgan, 2002); (b) simple unit cell and parameters of designation.

and Nijenhuis et al. (1991) have reported the heat of melting can reach a value of 100 J/g for a slow polymerization process yielding a highly crystalline stereospecific polymer.

Poly(L-lactide) can be crystallized into the α-form, β-form or γ-form, and this depends on the method of preparation and the thermal history. De Santis and Kovacs (1968) found that the conformation of the chain in the α-phase was a left-handed 10_7 helix for the L-isomer (PLLA), whereas it was a right-handed 10_3 for the D-isomer (PDLA) (see Figure 4.6). Both PLA chains have an orthorhombic unit cell of dimensions $a = 10.7$ Å, $b = 6.126$ Å and $c = 28.939$ Å. Based on the ratio of a and b parameters with a value of 1.737 (it is approximated to $\sqrt{3}$), it exhibits an almost hexagonal packing of helices. Hoogsten et al. (1990) suggested that the β-form of PLA was also in an orthorhombic unit cell, with parameters $a = 10.31$ Å, $b = 18.21$ Å and $c = 9.0$ Å, which accommodate six helices with a near-hexagonal packing (the b/a ratio is 1.76, i.e. $\approx\sqrt{3}$). In addition, Brizzolara et al. (1996) worked out that an orthorhombic unit cell based on a three-fold helix conformation with two parallel chains showed the existence of two distinct and interrelated phases. PLLA in the γ-form can be recovered through the epitaxial crystallization with two antiparallel s(3/2) helices in the pseudoorthorhombic unit cell ($a = 9.95$, $b = 6.25$, $c = 8.8$) exhibiting a three-fold helix conformation. Tsuji (2002) summarized unit cell parameters for non-blended and stereocomplex crystals and these are given in Table 4.3.

Table 4.3 Unit Cell Parameters for Non-Blended PLLA and Stereocomplex Crystals

Form	Space Group	Chain Orientation	No. of Helices/ Unit Cell	Helical Conformation	*a* (nm)	*b* (nm)	*c* (nm)	α (degree)	β (degree)	γ (degree)
PLLA α-form	Pseudo-orthorhombic	–	2	10_3	1.06	0.61	2.88	90	90	90
PLLA α-form	Orthorhombic	Parallel	2	10_3	1.05	0.61	–	90	90	90
PLLA α-form	Orthorhombic	–	6	3_1	1.031	1.821	0.90	90	90	90
PLLA α-form	Trigonal	Random up-down	3	3_1	1.052	1.052	0.88	90	90	120
PLLA α-form	Orthorhombic	Antiparallel	2	3_1	0.995	0.625	0.88	90	90	90
PLLA α-form	Triclinic	Parallel	2	3_1	0.916	0.916	0.870	109.2	109.2	109.8

Adapted from Auras et al., 2004.

4.3 Analytical Technique of PLA

4.3.1 Nuclear Magnetic Resonance Spectroscopy

PLA is formed by ring-opening polymerization of lactide, the cyclic dimer of lactic acid. In addition to the presence of stereoisomers of lactic acid, PLA properties are also influenced by the amount and distribution of L and D stereocenters of the polymer chains. Nuclear magnetic resonance (NMR) spectroscopy is playing an important role in determining the stereosequence distribution of the polymer. It is known that PLA with high stereoregularity can form highly crystalline polymers, i.e. isotactic PLA made up by either D-lactide or L-lactide has a higher rate of crystallization compared to meso-lactide, whichtends to form amorphous PLA when synthesized using nonstereoselective catalysts. NMR applies the principle that the magnetic nuclei in a magnetic field absorbs and re-emits electromagnetic radiation illustrating the tacticity of the structural orientation in the polymer.

The NMR spectrum exhibits resonances of particular polymers that possess stereosequence sensitivity. In the case of PLA, NMR spectra can distinguish the diads −LD− (or −DL−) and −LL− (or −DD−). But, the similar diads, −DD− and −LL−, or −LD− and −DL−, do not show different chemical shifts. In the stereosequence of PLA, the −DD− and −LL− produce an isotactic pairwise relationship, while −LD− and −DL− have the structure in a syndiotactic pairwise relationship. The observations from NMR have shown difficulties, such as overlaying of chemical shifts, insufficient resolution and probability of stereosequence formation due to polymer chains remaining in a huge macromolecule. For instance, for the stereosequence sensitivity of length n, there are $2^{(n-1)}$ possible combinations of pairwise relationships to be observed in NMR spectra.

Several studies have been conducted using NMR spectroscopy to determine the stereosequence distribution in PLA. Kricheldorf and Kreiser-Saunders (1990) has pioneered the use of methine resonance in ^{1}H and ^{13}C NMR spectra on various synthesis methods of PLA as well as the initiators/catalysts

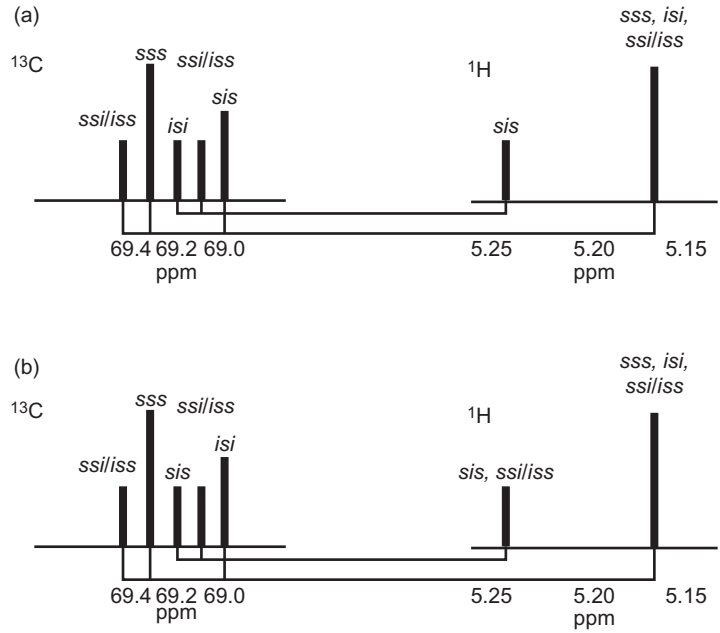

Figure 4.7 Comparison of the (a) Kricheldorf et al. (1996) and (b) Zell et al. (2002) tetrad stereosequence assignments of the methine carbon and proton in PLA synthesized using meso-lactide. The lines between peaks in the ^{1}H and ^{13}C NMR spectra indicate connectivity observed in the heteronuclear correlation NMR spectra (*i* designates isotactic, *s* designates syndiotactic).

involved. Meanwhile, Zell et al. (2002) has revised the tetrad stereosequence assignment for the methane carbon and proton of Kricheldorf et al. (1996) (see Figure 4.7). The revised tetrad stereosequence is an extension to the methine stereosequence assignments in PLA for upgrading to hexad level and includes a method for quantifying the amount of L-, D- and meso-lactide in PLA.

Figure 4.8 shows the ^{1}H and ^{13}C solution NMR spectra of PLA synthesized using 5% L-lactide and 95% D-lactide. As observed by Zell et al. (2002) in the ^{1}H spectrum, the direct integration of the *isi* resonance is impossible due to the overlapping of the *isi* resonance with the *iii* resonance. The ^{1}H and ^{13}C resonance relationship is shown in Figure 4.9. A similar situation can be found in the overlapping of the *sis* resonance

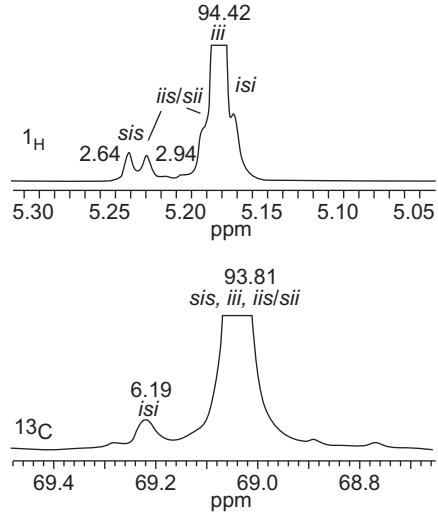

Figure 4.8 ^{1}H and ^{13}C solution NMR spectra of PLA synthesized using 5% L-lactide and 95% D-lactide (Zell et al., 2002).

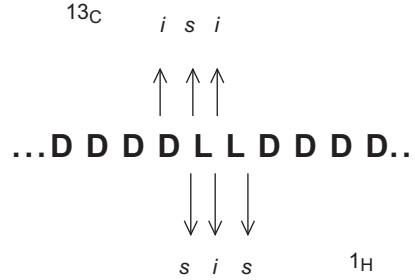

Figure 4.9 Direction of central pairwise relationship of ^{1}H and ^{13}C resonances (Zell et al., 2002).

with the *iii* resonance, which has caused no direct intergradations of the *sis* resonance. Zell et al. (2002) reported that the L-stereocenters from the L-lactide had at least four D stereocenters from D-lactide on either side in respect to the PLA synthesized using 5% L-lactide and 95% D-lactide with tin octanoate as an initiator in toluene at 70°C for 18 h.

Thakur et al. (1997) also conducted a study varying the composition of L-, D- and meso-lactide prepared by ring-opening

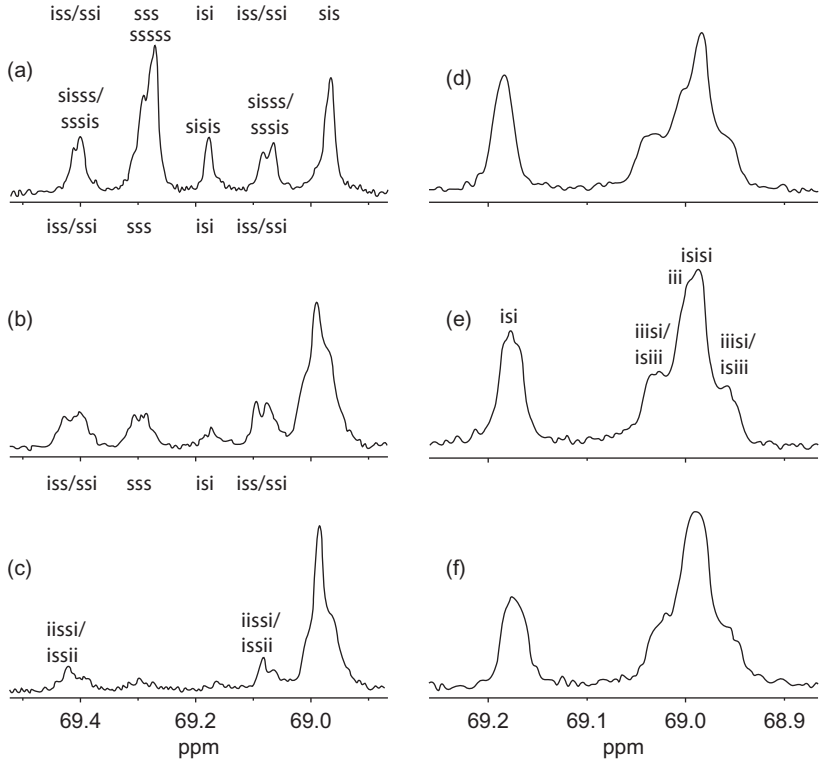

Figure 4.10 Methine resonances in the ^{13}C NMR spectra of PLA (a) 3:3:94 (% L-lactide:% D-lactide:% meso-lactide); (b) 51.5:1.5:47; (c) 70.9:0.9:28.2; (d) 50:50:0; (e) 60:40:0; (f) 70:30:0 (adapted from Thakur et al., 1997).

polymerization of lactides and catalyzed by tin (II) octanoate in a 1:10,0000 catalyst:monomer ratio, at 180°C for 3 h. The respective NMR spectra of the samples are shown in Figure 4.10. It can be observed that there is a preference for syndiotactic addition during the polymerization process, as inferred from the stereosequence distribution in the NMR spectra.

4.3.2 Infrared Spectroscopy

Infrared (IR) spectroscopy is an analytical method to determine the presence of functional groups and unveil the bonding

Table 4.4 The Infrared Spectroscopy Wavenumber Corresponding to the Bonding and Functionality in PLA

Assignment	Wavenumber (cm^{-1})
–OH stretch (free)	3100
–CH–stretch	2997 (asymmetric), 2946 (symmetric), 2877
–C=O carbonyl stretch	1748
$–CH_3$ bend	1456
–CH–deformation including symmetric and asymmetric bend	1382, 1365
–C=O bend	1225
–C–O–stretch	1194, 1130, 1093
–OH bend	1047
$–CH_3$ rocking modes	956, 921
–C–C–stretch	926, 868

Adapted from Auras et al., 2004.

or interactions within the substance. The IR spectrum of a polymer is normally analyzed using the Fourier transform infrared spectroscopy (FT-IR) method with the scans normally done at 4000–400 cm^{-1}, with results provided in percentage transmission or absorbance. IR spectroscopy picks up the vibrations of bonds and provides evidence of functional groups. Stronger bonds are generally stiffer, requiring greater forces to stretch or compress them. Peak assignments for PLA (98% L-lactide) of IR spectra are summarized in Table 4.4. As shown in Figure 4.11, the most important indication of PLA is the presence of –C=O carbonyl stretch at 1748 cm^{-1} and –C=O carbonyl bending at 1225 cm^{-1}. There are three stretching bands for –C–H, denoted by 2997 cm^{-1} for asymmetric, 2945 cm^{-1} for symmetric and 2877 cm^{-1}. The lowest wavenumber, 2877 cm^{-1}, is assigned for the methyl $–CH_3$, which has weaker bonding. However, when the oxygen atom is next to C–H, the wavenumber will increase due to the electronegativity of the atom strengthening C–H. As a result, the O=C–H is assigned the wavenumber 2997 cm^{-1}. The –OH

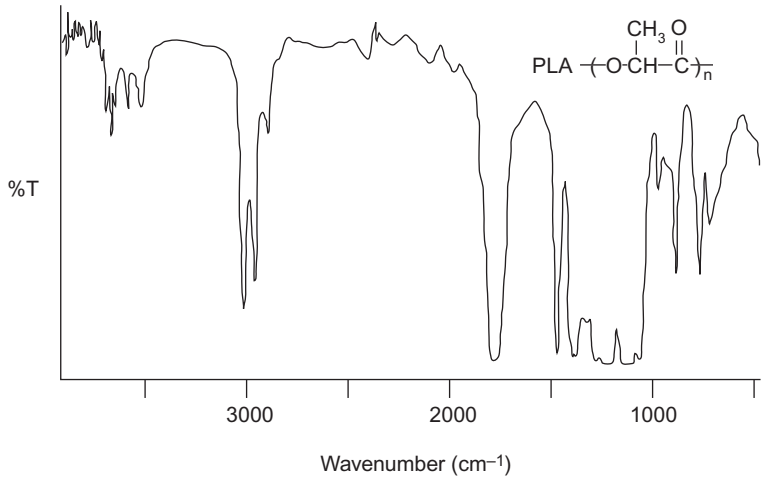

Figure 4.11 Infrared spectrum for PLA composed of 95% L-lactide, 5% meso-lactide, with average molecular weight (M_w) of 9.73×10^4.

stretching band at 3571 cm^{-1} is a broad band, which is also characteristic of carboxylic acid. The —OH stretching band of carboxylic acid is lower than for alcohol (3300 cm^{-1}) due to the unusually strong hydrogen bonding in carboxylic acids. The bending mode corresponds to —C═O and —OH and can be found at 1225 cm^{-1} and 1047 cm^{-1}, respectively. However, the band at the lower wavenumber tends to show overlapping, leading to difficulty in characterization.

Recently, Pan et al. (2011) conducted a study using the FT-IR technique to investigate the crystalline structure of PLLA and PLLA/PDLA stereocomplex. PLA tends to form various crystal polymorphisms depending on the crystallization conditions. The usual polymorph, α-form, is crystallized by the cold, melt or solution route, yielding an orthorhombic (or pseudo-orthorhombic) unit cell in a distorted 10_3 conformation (Aleman et al., 2001). When the α counterpart is stretched at a high temperature to a high drawing ratio, the PLA will transform into the β-form, which adopts a 3_1 helical conformation (Sawai et al., 2003). Another metastable α′-form is attained from the stereoregular PLA melt-crystallined at a low crystallization temperature T_c (<100°C), whereas the α-form is yielded

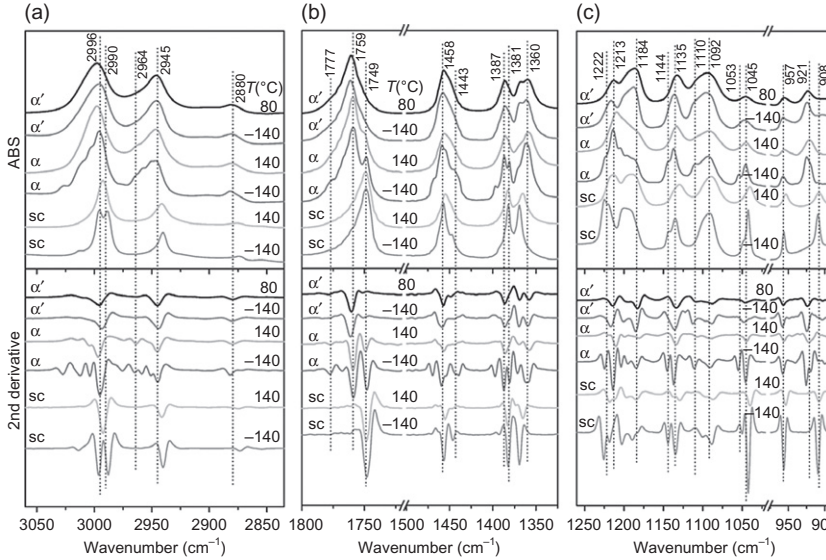

Figure 4.12 Temperature-dependent FT-IR spectra and their second derivatives of α′, α and amorphous (sc) forms of PLA. Intensities of FT-IR spectra and their second derivatives in the wavenumber ranges 1500−1325 and 975−890 cm^{-1} were magnified for clarity. ABS = absorbance (adapted from Pan et al., 2011).

at higher T_c (>120°C) (Zhang et al., 2005a). Pan et al. (2011) found that the α-form PLA showed spectral splitting (see Figure 4.12). The α-form PLA spit into a few new peaks when cooled to −140°C: −3006 cm^{-1} (CH_3 asymmetric stretching), 2964 cm^{-1} (CH_3 symmetric stretching), 1777 and 1749 cm^{-1} (C═O stretching), 1468 and 1443 cm^{-1} (CH_3 asymmetric bending), 1396 and 1381 cm^{-1} (CH_3 symmetric bending), 1222 cm^{-1} (C−O−C asymmetric bending and CH_3 asymmetric rocking), 1144 cm^{-1} (CH_3 asymmetric rocking), and 1053 cm^{-1} (C−CH_3 bending). The α′ crystal has remarkable result compared to the former without exhibiting spectral splitting. This is because the α′ crystal has weaker interchain interactions in its crystal lattice. In other words, there is lack of lateral interactions between the molecular chains contained in a crystal unit cell. When a comparison was made for the blend of PLLA/PDLA, which was in the amorphous structure,

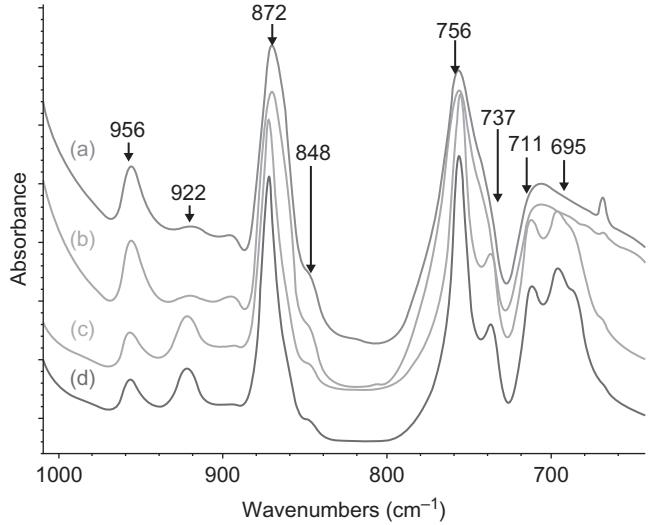

Figure 4.13 Infrared spectra of neat PLLA at various annealing temperatures in the region 1000−600 cm^{-1}: (a) room temperature 25°C, (b) 80°C, (c) 110°C and (d) 140°C (Vasanthan et al., 2011).

it showed that the corresponding peak for C═O stretching is about 10 cm^{-1} lower, while CH_3 asymmetric/symmetric stretching and CH symmetric stretching is reduced by 4−6 cm^{-1}. It can, therefore, be assumed that weak hydrogen bonds form in C−H− − − −O═C in the amorphous PLA crystal (Zhang et al., 2005b).

Figure 4.13 shows the IR spectra of PLLA films annealed at room temperatures of 80−120°C at the region of 1000−650 cm^{-1}, which were done to investigate the spectral differences between semicrystalline and amorphous PLLA. The PLLA films annealed at higher temperatures possess higher crystallization due to the increase in temperature-enabled flexible chain movement, which promotes crystallization rearrangement. The spectra of the annealed PLA have distinct differences, with few peaks at 956, 922, 872, 848, 756, 737, 711 and 695 cm^{-1}. It is obvious that the IR spectra of semicrystalline and of amorphous PLLA have distinct differences. It can be observed that when annealed at higher temperatures, the bands shift to higher wavenumbers. This is due to the fact that

crystallization limits the vibration of bonding. For instance, the vibration of −COOH as assigned to the band at 956 cm^{-1} is shifted by a reduction of 5−8 cm^{-1} when the annealing temperature is higher. It has also been noted that the band at 956 cm^{-1} decreases in intensity (or absorbance) while the band at 922 cm^{-1} increases in intensity with increasing annealing temperature. The band at 922 cm^{-1} represents the combination of C−C backbone and CH_3 rocking mode of PLLA crystals (Zhang et al, 2005b). The bands at 872 and 848 cm^{-1} become weaker as the annealing temperature increases. The bands at 737 and 717 cm^{-1} appeared as a single band in the IR spectrum and both bands split into two bands as the annealing temperature exceeds 100°C. The splitting of the band can be explained by the formation of a multiphase related to the presence of crystal and amorphous regions. As a result, the split is into the higher band, which is assigned to crystal region functionality, and the lower band, which represents the functional group in the amorphous region. The prescribed functional group of the splitting of the band belongs to the bending/rocking mode of $-CH_3$.

4.4 Solubility and Barrier Properties of PLA

PLA is a suitable biopolymer to replace conventional petrochemical polymers as packaging materials. The 'green' characteristics of PLA have been 'eye-opening' in the food packaging industry, as it has good barrier properties in maintaining the freshness of food while not polluting the environment. Careful selection of packaging material by food producers is extremely important to avoid chemical and biological contamination, and the rapid spoilage of food. Packaging materials must provide a sufficient barrier against water vapor to prevent food degradation or the growth of microorganisms, prevent the permeation of atmospheric gases what would initiate oxidation, and maintain the volatile organic compounds contained in the food to preserve the aromas and flavors. Moreover, packaging should be insoluble in many types of solvents to avoid the migration

of packaging traces into the food, which could endanger health when consumed.

In general, the possibility of food contamination or poisoning from PLA containers used in the market is low. This is because PLA is produced from the lactide monomer, which is originated from L-lactic acid, a nontoxic component that exists naturally in the human body. Nevertheless, the presence of trace levels of D-lactic acid, a minor side-product during polymerization, is possible. D-lactic acid cannot be consumed by the human body, due to the lack of an appropriate enzyme. The determination of the permeability (solubility and diffusion) of gases, flavors and aromas in polymers is of vital importance in the application of PLA in the food packaging industry. This is discussed in the next section. The method of determining levels of D-lactic acid and lactide for safety purposes are discussed in Chapter 2, and this is an important aspect of the application of PLA as packaging material.

4.4.1 Solubility of Polylactic Acid

According to Nampoothiri et al. (2010), PLA can be dissolved in chloroform, methylene chloride, dioxane, acetonitrile, 1,1,2-trichloroethane and dichloroacetic acid. PLA can also be soluble in toluene, acetone, ethyl benzene and tetrahydrofuran (THF) when heated to boiling temperatures, but its solubility is limited at low temperatures. Generally, no PLA can be dissolved in water, selective alcohols and alkanes. Highly crystalline PLLA resists solvent attack of acetone, ethyl acetate and tetrahydrofuran, whereas amorphous PLA, such as the copolymer of poly (L,D-lactide), can be easily dissolved in various organic solvents, such as THF, chlorinated solvents, benzene, acetonitrile and dioxane.

The solubility of PLA depends on the crystallinity of the polymer because a highly oriented structure increases the difficulty of interchain migration of solvent molecules. The principle of thermodynamic criterion of solubility is based on the free energy of mixing (ΔG_M), which states that two substances are mutually soluble if ΔG_M is zero or negative. The free

energy of mixing for a solution process between a solvent and a polymer is related as: $\Delta G_M = \Delta H_M - T\,\Delta S_M$, where ΔH_M, T, and ΔS_M are the enthalpy of mixing, absolute temperature and entropy of mixing, respectively. Normally the value of ΔS_M is small and positive. Thus, the solubility of solvents greatly depend on the ΔH_M and T. The solubility of a substance is represented by solubility parameter (δ), which was introduced by Hildebrand and Scott (1950), and is related to the cohesive energy density. Hansen and Skaarup (1967) later proposed solubility parameters linked with polarity and the hydrogen bonding system, which was divided into three components, namely non-polar (δ_D), polar (δ_p) and hydrogen bond (δ_h), where the Hansen solubility parameter, $\delta_T = \delta_D + \delta + \delta_k$. Table 4.5 and Table 4.6 summarize the solubility parameters for solvents and PLA, respectively. In order to dissolve PLA in a solvent, the solubility parameters of the polymer and solvent should have a difference of $\delta_t < 2.5$ (Auras, 2007). The liquid components contained in food, such as water, ethanol and paraffin (as represented by hexane), have greater differences of solubility parameters than PLA; thus PLA is safe to be in contact with food without the possibility of migration.

Auras (2007) computationally compared the solubility of PLA, polyethylene terephthalate (PET) and polystyrene (PS) using regular solution theory (RST) for various solvents. As can be seen from Figure 4.14, the solubility regions of PLA, PET, and PS can be approximated by a boundary of radius $\sim 2.5\delta$ unit from the value of PLA ($\delta_v = 19.01$, $\delta_H = 10.01$), PET ($\delta_v = 19.77$, $\delta_H = 10.97$) and PS ($\delta_v = 15.90$, $\delta_H = 5.00$). Nevertheless, the solubility of the polymers declines when the distance of solvents is large. It can be concluded from the results that both PLA and PET have similar solubility properties, and so both can be used interchangeably.

4.4.2 Permeability of Polylactic Acid

The gas permeation properties of PLA are important when considering it as a packaging material. Packaging requires low permeability materials, to avoid the loss of flavor, aroma or the

Table 4.5 Solubility Parameters of Solvents at 25°C (Hansen, 2000)

Solvent	Hansen Solubility Parameter, δ_T (J/cc)$^{0.5}$ at 25°C			
	δ_d[a]	δ_p[a]	δ_h[a]	δ_t
Acetone	15.0	10.4	7	19.6
Acetonitrile	15.3	18.0	6.1	24.4
Benzene	18.4	0.0	2.0	18.5
Chloroform	17.8	3.1	5.5	18.9
m-Cresol	18	5.1	12.9	22.7
Dimethyl formamide	17.4	13.7	11.3	24.9
Dimethyl suphoxide	18.4	16.4	10.0	26.6
1-4 Dioxane	19.0	1.8	7.4	20.5
1-3 Dioxolane	18.1	6.6	9.3	21.4
Ethyl acetate	15.8	5.3	7.2	18.2
Furan	17.8	1.8	5.3	18.7
Hexafluoro isopropanol	17.2	4.5	14.7	23.1
Isoamyl alcohol	15.8	5.2	13.3	21.3
Methylene dichloride	18.2	6.3	6.1	20.2
Methyl ethyl ketone	16.0	9.0	5.1	19.1
n-Methyl pyrolidone	18.0	12.3	7.2	23.0
Pyridine	19.0	8.8	5.9	31.8
Tetrahydrofuran	16.8	5.7	8.0	19.5
Toluene	18.0	1.4	2.0	18.2
Xylene	17.6	1.0	3.1	17.9
Nonsolvents				
Isopropyl ether	13.7	3.9	2.3	14.4
Cyclohexane	16.5	0.0	0.2	16.5
Hexane	14.9	0.0	0.0	14.9
Ethanol	15.8	8.8	19.4	26.5
Methanol	15.1	12.3	22.3	29.6
Water	15.5	16.0	42.3	47.8
Diethyl ether	14.5	2.9	5.1	15.6

Table 4.6 Solubility Parameters for PLA at 25°C (See Agrawal et al., 2004, for Calculation Method)

Method	δ_d $(J/cc)^{0.5}$	δ_p $(J/cc)^{0.5}$	δ_h $(J/cc)^{0.5}$	δ_t $(J/cc)^{0.5}$
Intrinsic 3D viscosity	17.61	5.30	5.80	19.28
Intrinsic 1D viscosity	–	–	–	19.16
Classical 3D geometric	16.85	9.00	4.05	19.53
Fedors group contribution	–	–	–	21.42
Van Kreveln group contribution	–	–	–	17.64

occurrence of oxidation, all of which can shorten the shelf life of food. Because PLA is a biodegradable material with the potential to substitute existing plastic materials, such as PET, PS and low-density polyethylene (LDPE), it is very important for PLA to have as effective permeability characteristics as these existing polymers.

Lehermeier et al. (2001) conducted a study on the gas permeation of PLA for nitrogen, oxygen, carbon dioxide and methane. The results are summarized in Table 4.7. The activation energy of permeation (E_p) can be calculated as follows:

$$P = P_o \exp\left(-\frac{E_p}{RT}\right) \tag{4.1}$$

It was observed that the permeability of PET was lower than PLA. In other words, PET has superior barrier properties than PLA with an L:D ratio of 96:4. Lehermeier et al. (2001) concluded that this is due to PET containing aromatic rings in the polymer chain backbone, which reduces free volume and chain mobility. There is a lack of significant change with the introduction of branching in the PLA chains. However, crystallization can greatly improve the barrier properties. The increment of crystallinity in biaxially orientated PLA film (L:D ratio of 95:5) with 16% crystallinity caused the permeability to reduce 4.5 times less than PLA film samples (with L:D of 96:4 and 98:2) having 1.5% and 3% crystallinity, respectively. This is

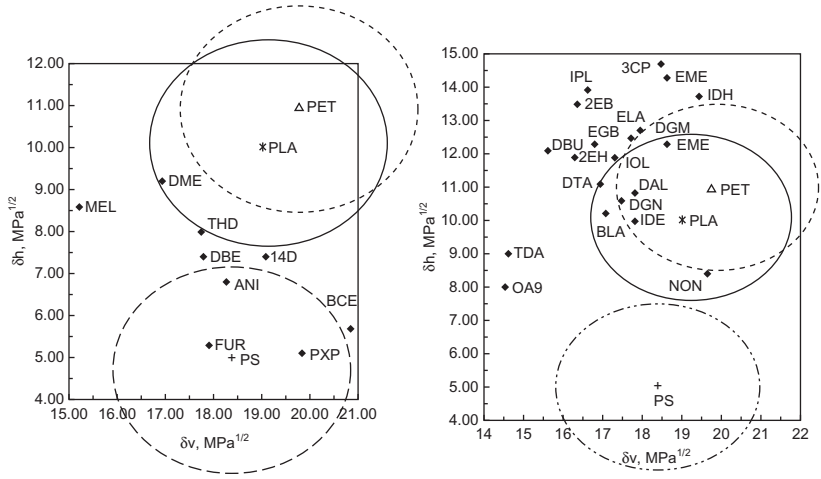

Figure 4.14 (a) Volume-dependent cohesion parameter (δ_v) versus Hansen hydrogen-bonding parameter (δ_h) for PLA. Values indicated for solvents with $\Delta\delta < 5$ MPa$^{1/2}$: FUR = furan; EPH = epichlorohydrin; THD = tetrahydrofuran; 14D = 1,4-dioxane; MEL = methylal (dimethoxymethane); BCE = bis(2-chloroethyl) ether; ANI = anisole (methoxybenzene); DME = di-(2-methoxyethyl) ether; DBE = dibenzyl ether; PXP = bis-(m-phenoxyphenol) ether; 3CP = 3-chloropropanol; BEA = benzyl alcohol; CHL = cyclohexanol; 1PL = 1-pentanol; 2EB = 2-ethyl-1-butanol; DAL = diacetone alcohol; DBU = 1,3-dimethyl-1-butanol; ELA = ethyl lactate; BLA = n-butyl lactate; EME = ethylene glycol monoethyl ether; DGM = diethylene glycol monoethyl ethermethyl; DGE = diethylene glycol monoethyl ether; EGB = ethylene glycol mono-n-butyl ether; 2EH = 2-ethyl-1-hexanol; IOL = 1-octanol; 2OL = 2-octanol; DGN = diethylene glycol mono n-butyl ether; 1DE = 1-decanol; TDA = 1-tridecanol; NON = nonyl; OA9 = oleyl alcohol (adapted from Auras, 2007).

because crystallinity improves the compaction of structure, leading to a difficulty for gas molecules to diffuse through the film. A comparison of the permeation properties of 100% linear PLA possessing an L:D ratio in line with other commodity polymers mainly for packaging are shown in Figure 4.15. The data is self-explanatory: PLA possesses good barrier properties compared to PS and LDPE. PLA has been shown to have preferential barrier properties in relation to nitrogen, carbon dioxide and methane, but slightly weaker barrier properties for

Table 4.7 Permeation Properties of PLA and PET

Gas	Polymer	Permeability at 25°C ($\times 10^{-10}$ cm^3 (STP).cm/cm^2.s.cm.Hg)	Activation (kJ/mol)	Temperature Dependence Permeation, P_T ($\times 10^{-10}$ cm^3 (STP).cm/cm^2.s.cm.Hg)
Nitrogen	Linear PLA L:D (96:04)	1.3	11.2	$P_T = 109.86\ e^{-1.36X}$
	Linear PLA L:D (98:02)			–
	PET	0.008[a]	26.4[b]	–
Oxygen	Linear PLA L:D (96:04)	3.3	11.1	$P_T = 276.43\ e^{-1.34X}$
	Linear PLA L:D (98:02)			–
	PET	0.04[a]	37.7[b]	–
Carbon dioxide	Linear PLA L:D (96:04)	10.2	6.1	$P_T = 115.67\ e^{-0.78X}$
	Linear PLA L:D (98:02)			–
	PET	0.2[a]	27.6[b]	–
Methane	Linear PLA L:D (96:04)	0.9	13.0	$P_T = 149.95\ e^{-1.55X}$
	Linear PLA L:D (98:02)	0.8	–	–
	Biaxially oriented film L:D (95:05)	0.19	–	–
	PET	0.004[a]	24.7[b]	–

a = Michaels et al. (1963); b = Pauly (1999); $X = 1/T \times 10^3$/K.
Adapted from Lehermeier et al., 2001.

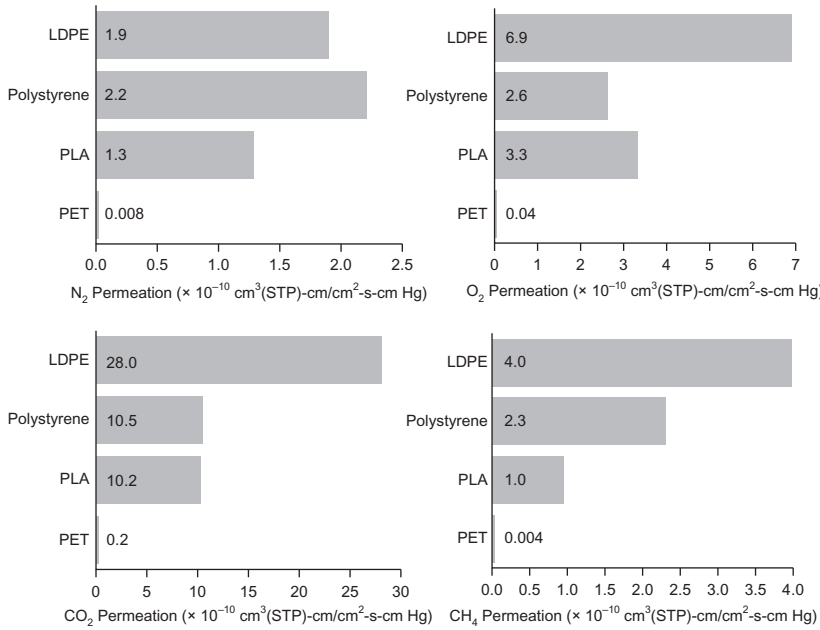

Figure 4.15 Permeation properties of 100% linear PLA having a L:D ratio of 96:04 compared to other common plastics at 30°C (adapted from Lehermeier et al., 2001).

oxygen. This finding is important, in that it shows that PLA can be utilized as a robust packaging material to substitute various commodity petrochemical-based plastic films. Its good barrier properties, along with its biodegradability and 'green' production, mean that PLA is a strong contender as a future packaging material.

Permeability to water is another important factor that needs to be considered for packaging materials. Shogren (1997) compared the water vapor permeability of various biodegradable polymers, including poly(β-hydroxybutyrate-co-hydroxyvalerate) (PHBV) containing 6, 12 and 18% valerate, poly(ε-caprolactone) (PCL), amorphous and crystalline poly(L-lactic acid), etc. The water transmission rates for these materials as established by Shogren are presented in Table 4.8. PLA exhibits good water resistance in comparison to many biodegradable polymers except PHBV. Moreover, annealing of PLA at 130°C

Table 4.8 Water Vapor Transmission Rates of Biodegradable Polymer Films (Shogren, 1997)

Film	Water Vapor Transmission Rate ($g/m^2/day$)			Crystallinity (%)	Solubility Parameter $(J/cm^3)^{1/2}$
	T = 6°C	T = 25°C	T = 49°C		
PHBV-6	1.8	13	124	74	21.5
PHBV-12	3.1	21	204	69	21.5
PHBV-18	3.5	26	245	62	21.4
PLA-crystalline	27	82	333	66	22.7
PLA-amorphous	54	172	1100	0	22.7
PCL	41	177	1170	67	20.8
Bionolle	59	330	2420	0	–
BAK 1095	134	680	3070	0	–
CAP	590	1700	5200	41	24.2
CA	1020	2920	7900	33	25.7

PHBV = poly(β-hydroxybutyrate-co-hydroxyvalerate) with 6, 12 and 18% valerate; PLA-cystalline = PLA annealed at 130°C; PCL = poly(ε-caprolactone); CA = cellulose acetate; CAP = cellulose acetate propionate; Bionelle = blown film containing an aliphatic polyester; BAK 1095 = blown film containing poly(ester-amide). Solubility parameter for water is 47.9 $(J/cm^3)^{1/2}$.

induces the formation of a crystalline structure, which improves water resistivity. This can be explained by the fact that crystallization reduces the molecular cross-sectional area for diffusion and increases the diffusion path length by imposing restraints on the mobility of the amorphous phase (Shogren, 1997). Similarly, the solubility parameters of the polymers also greatly influence water vapor permeability. When the difference between the solubility parameter value for a polymer and water is small, this means that the polymer favors water, thus, the transmission rate is higher.

Siparsky et al. (1997) performed an depth investigation on the effect of copolymerization on water transmission of PLA film. The 'solution-diffusion' model (Equation 4.2) was used to

Table 4.9 Diffusion, Solubility, and Permeability Coefficients of PLA, PCL and its Copolymers/Blends, Measured at 90% Relative Humidity and Temperature of 20°C (Siparksy et al., 1997)

Composition	T_g (°C)	% crystallinity	P ($\times 10^{13}$)	S ($\times 10^{6}$)	D ($\times 10^{6}$)
50:50 L:D PLA	52	–	2200	3400	0.067
70:30 L:D PLA	50	–	2200	2200	0.10
90:10 L:D PLA	54	–	1500	2000	0.078
95:5 L:D PLA	59	–	1400	3000	0.044
100:0 L:D PLA (quenched)	63	11	1900	4000	0.052
100:0 L:D PLA	63	39	1600	4000	0.046
100:0 L:D (annealed 15 min at 160°C)	63	46	2000	4000	0.040
30% random PCL: PLA	40	PCL<5	2900	2200	0.13
30% block PCL: PLA	−63, 47	PCL: 9	3100	3100	0.10
30% oriented PCL: PLA	−63, 43	PCL: 11	2700	2600	0.11
PCL	−60	52	3200	1600	0.20
20% blend polyethylene glycol with PLA	48	–	5700	10900	0.052

P is in units of cm^3 (STP) cm/cm^2 s Pa; S is in units of cm^3 (STP) cm^3 Pa; D is in unit of cm^2/s.

characterize the water vapor in PLA. P is the permeability coefficient relates to flux, S is the solubility coefficient representing the equilibrium water concentration and D is diffusion coefficient relates to diffusivity.

$$\text{Solution Diffusion Model: } P = S \times D \tag{4.2}$$

Table 4.9 exhibits the diffusivity of water vapor as affected by the composition of L:D in PLA. A stereospecific isomer of PLA has a better water vapor barrier resistance due to its

oriented structure. Nevertheless, the crystallinity of PLA showed a lack of influence on the permeability to water vapor. Incorporation of caprolactone monomers have a moderate effect on the diffusivity, but the blending of polyethylene glycol (PEG) caused a dramatic drop in water vapor resistance. The hydrophilicity of PEG, as well as the disruption of structure, are factors that caused this reduction in barrier properties when combined with PLA.

4.5 Conclusion

The properties of PLA are significantly influenced by the stereochemistry of its monomers. When PLA has high stereochemical purity, it tends to form a highly crystalline structure. Copolymerization of different lactide isomers can yield a variety characteristics of PLA. The effect of isomerization in PLA can be detected by IR and NMR spectroscopic methods. Many studies have proven that PLA has a low solubility in a wide range of solvents/liquids, such as water, alcohol and paraffin. This indicates that PLA can be safely employed as a food packaging material without causing adverse health effects. In addition, PLA also possesses barrier properties that are just as effective as LDPE and PS. The 'green' aspect of PLA means that it represents a viable environmentally friendly substitute for petrochemical-based polymers.

References

Agrawal, A., Saran, A.D., Rath, S.S., Khanna, A., 2004. Constrained nonlinear optimization for solubility parameters of poly(lactic acid) and poly(glycolic acid)- validation and comparison. Polymer 45, 8603–8612.

Aleman, C., Lotz, B., Puiggali, J., 2001. Crystal structure of the α-form of poly(L-lactide). Macromolecules 34, 4795–4801.

Auras, R.A., 2007. Solubility of gases and vapors in polylactide polymers. In: Letcher, T.M. (Ed.), Thermodynamics, Solubility and Environmental Issues. Elsevier, The Netherlands, pp. 343–368.

Auras, R.A., Harte, B., Selke, S., 2004. An overview of polylactides as packaging materials. Macromol. Biosci. 4, 835–864.

Brizzolara, D., Cantow, H.-J., Diederichs, K., Keller, E., Domb, A.J., 1996. Mechanism of the stereocomplex formation between enantiomeric poly(lactide)s. Macromolecules 29, 191–197.

Dahlman, J., Rafler, G., Fechner, K., Mechlis, B., 1990. Synthesis and properties of biodegradable aliphatic polyesters. Br. Polym. J. 23, 235–240.

De Santis, P., Kavacs, A.J., 1968. Molecular conformation of poly(S-lactic acid). Biopolymer 6, 299–306.

Drumlight, R.E., Gruber, P.R., Henton, D.E., 2000. Polylactic acid technology. Advan. Mater. 12, 1841–1846.

Garlotta, D., 2002. A literature review of poly(lactic acid). J. Polym. Environ. 9, 63–84.

Hartmann, H., 1998. High molecular weight polylactic acid polymers. In: Kaplan, D.L. (Ed.), Biopolymers from Renewable Resources. Springer-Verlag, Berlin, pp. 367–411.

Hansen, C.M., 2000. Hansen solubility parameters—a user's handbook. CRC Press, Florida.

Hansen, C.M., Skaarup, K., 1967. Three dimensional solubility parameter – key to paint component affinities: III. Independent calculation of the parameter components. J. Paint Technol. 39, 511–514.

Henton, D.E., Gruber, P., Lunt, J., Randall, J., 2005. Polylactic acid technology. In: Mohanty, A.K., Misra, M., Drzal, L.T. (Eds.), Natural Fibers, Biopolymers, and Biocomposites. Taylor & Francis, Boca Raton, FL, pp. 527–577.

Hildebrand, J.H., Scott, R.L., 1950. The Solubility of Nonelectrolytes. Reinhold Pub. Corp., New York.

Hoogsten, W., Postema, A.R., Pennings, A.J., ten Brinke, G., Zugenmaier, P., 1990. Crystal structure, conformation and morphology of solution-spun poly(L-lactide) fiber. Macromolecules 23, 634–642.

Huang, J., Lisowski, M.S., Runt, J., Hall, E.S., Kean, R.T., Buehler, N., et al., 1998. Crystallization and microstructure of Poly(L-lactide-co-meso-lactide) copolymer. Macromolecules 31, 2593–2599.

Ikada, Y., Jamshidi, K., Tsuji, H., Hyon, S.H., 1987. Stereocomplex formation between enantionmeric poly(lactides). Macromolecules 20, 904–906.

Iwata, T., Doi, Y., 1998. Morphology and enzymatic degradation of poly (L lactic acid) single crystals. Macromolecules 31, 2461–2467.

Jain, R.J., 2000. The manufacturing techniques of various drug loaded biodegradable poly(lactide-co glycolide) (PLGA) devices. Biomaterials 21, 2475–2490.

Kolstad, J.J., 1996. Crystallization kinetics of poly(L-lactide-co-mesolactide). J. Appl. Polym. Sci. 62, 1079–1091.

Kricheldorf, H.R., Boettcher, C., 1993. Polylactones. XXV. Polymerizations of racemic- and meso-D, L-lactide with Zn, Pb, Sb, and Bi salts- Stereochemical aspects. J. Macromolecular Sci., Part A: Pure and Appl. Chem. 30, 441–448.

Kricheldorf, H.R., Kreiser-Saunders, I., 1990. Polylactones, 19. Aninic polymerization of L-lactide in solution. Die Makromolekulare Chem. 191, 1057–1066.

Kricheldorf, H.R., Kreiser-Saunders, I., Jürgens, C., Wolter, D., 1996. Polylactides- synthesis, characterization and medical application. Macromol. Symp. 103, 85–102.

Lehermeier, J.J., Dorgan, J.R., Way, D.J., 2001. Gas permeation properties of poly(lactic acid). J. Memb. Sci. 190, 243–251.

Lunt, J., 1998. Large scale production, properties and commercial applications of polylactic acid polymers. Polym. Degrad. Stabil. 59, 145–152.

Lunt, J., Shafer, A.L., 2000. Polylactic acid polymers from corn: applications in the textiles industry. J. Ind. Text 29, 191–205.

Michaels, A.S., Vieth, W.R., Barrie, J.A., 1963. Diffusion of gases in polyethylene terephthalate. J. Appl. Phys. 34, 13–20.

Morgan, E., 2002. Left and right hand helices. Accessed from <http://wbiomed.curtin.edu.au/biochem/>.

Mutsuga, M., Kawamura, Y., Tanamoto, K., 2008. Migration of lactic acid, lactide and oligomers from polylactide food-contact materials. Food Addit. Contam.- Part A Chem., Anal., Control, Expo. Risk Assess. 25, 1283–1290.

Nampoothiri, K.M., Nair, N.R., John, R.P., 2010. An overview of the recent developments in polylactide (PLA) research. Bioresour. Technol. 101, 8493–8501.

Nijenhuis, A.J., Grijpma, D.W., Pennings, A.J., 1991. Highly crystalline as-polymerized poly(l-lactide). Poly. Bull. 26, 71–77.

Ovitt, T.M., Coates, G.W., 1999. Stereoselective ring-opening polymerization of meso-lactide: Synthesis of syndiotactic poly(lactic acid). J. Am. Chem. Soc. 121, 4072–4073.

Ovitt, T.M., Coates, G.W., 2000. Stereoselective ring-opening polymerization of *rac*-lactide with single-site, racemic aluminum alkoxide catalyst: synthesis of stereoblock poly(lactic acid). J. Polym. Sci., Part A: Polym. Chem. 38, 4686–4692.

Pan, P., Yang, J., Shan, G., Bao, Y., Weng, Z., Cao, A., et al., 2011. Temperature-variable FTIR and solid-state ^{13}C NMR investigations on crystalline structure and molecular dynamics of polymorphic poly(L-lactide) and poly(L-lactide)/poly(D-lactide) stereocomplex. doi: 10.1021/ma201906a.

Pauly, S., 1999. Permeability and diffusion data. In: Brandrup, J., Immergut, E.H., Grulke, E.A. (Eds.), Polymer Handbook, fourth ed. Wiley, New York, pp. 543–569.

Reddy, G., Altaf, M., Naveena, B.J., Venkateshwar, M., Kumar, E.V., 2008. Amylolytic bacterial lactic acid fermentation – a review. Biotechnol. Adv. 26, 22–34.

Sawai, D., Takahashi, K., Sasashige, A., Kanamoto, T., Hyon, S.-H., 2003. Preparation of oriented β-form poly(L-lactic acid) by solid-state coextrusion: effect of extrusion variables. Macromolecules 36, 3601–3605.

Shogren, R., 1997. Water vapor permeability of biodegradable polymers. J. Environ. Polym. Degrad. 5, 91–95.

Siparsky, G.L., Voorhees, K.J., Dorgan, J.R., Schilling, K., 1997. Water transport in polylactic acid (PLA), PLA/Polycaprolactone copolymers, and PLA/Polyethylene glycol blends. J. Environ. Polym. Degrad. 5, 125–136.

Thakur, K.A.M., Kena, R.T., Hall, E.S., Kolstad, J.J., Lindgren, T.A., 1997. High-resolution ^{13}C and ^{1}H solution NMR study of poly(lactide). Macromolecules 30, 2422–2428.

Tsuji, H., 2002. Polylactides. In: Doi, Y., Steinbüchel, A. (Eds.), Biopolymers. Polyesters III. Applications and Commercial Products. Wiley-VCH Verlag GmbH, Weinheim, pp. 129–177.

Tsuji, H., Ikada, Y., 1995. Properties and morphologies of poly(l-lactide): 1. Annealing condition effects on properties and morphologies of poly(l-lactide). Polymer 41, 8921–8930.

Tsuji, H., Ikada, Y., 1996. Blends of isotactic and atactic poly(lactide)s: 2. Molecular-weight effects of atactic component on crystallization and morphology of equimolar blends from the melt. Polymer 37, 595–602.

Tsuji, H., Ikada, Y., 1999. Stereocomplex formation between enantionmeric poly(lactic acids)s. XI. Mechanical properties and morphology. Polymer 40, 6699–6708.

Urayama, H., Kanamori, T., Fukushima, K., Kimura, Y., 2003. Controlled crystal nucleation in the melt crystallization of poly (L-lactide) and poly(L-lactide)/poly(D-lactide) stereocomplex. Polymer 44, 5635–5641.

Vasanthan, N., Ly, H., Ghosh, S., 2011. Impact of nanoclay on isothermal cold crystallization kinetics and polymorphism of poly(L-lactide acid) nanocomposites. J. Phys. Chem. B 115, 9556–9563.

Yui, N., Dijkstra, P., Feijen, J., 1990. Stereo block copolymers of L- and D-lactides. Macromolecule Chem. 191, 487–488.

Zell, M.T., Padden, D.E., Paterick, A.J., Thakur, K.A.M., Kean, R.T., Hillmyer, M.A., et al., 2002. Unambiguous determination of the 13C and 1H NMR stereosequence assignments of polylactide using high-resolution solution NMR spectroscopy. Macromolecules 35, 7700–7707.

Zhang, J., Duan, Y., Sato, J., Tsuji, H., Noda, I., Wan, S., et al., 2005a. Crystal modifications and thermal behavior of poly(L-lactic acid) revealed by infrared spectroscopy. Macromolecules 38, 8012–8021.

Zhang, J., Sato, H., Tsuji, J., Noda, I., Ozaki, Y., 2005b. Infrared spectroscopic study of CH_3-OC interaction during poly(L-lactide)/poly(D-lactide) stereocomplex formation. Macromolecules 38, 1822–1828.